Modeling of molecular photocells: Application to two-level photovoltaic system with electron-hole interaction

Tahereh Nemati Aram,[1,2,a)] Petrutza Anghel-Vasilescu,[1] Asghar Asgari,[2,3]
Matthias Ernzerhof,[4] and Didier Mayou[1]
[1]*Institut Néel, CNRS and Université Grenoble Alpes, Grenoble F-38042, France*
[2]*Research Institute for Applied Physics and Astronomy, University of Tabriz, Tabriz 51665-163, Iran*
[3]*School of Electrical, Electronic and Computer Engineering, The University of Western Australia, Crawley, WA 6009, Australia*
[4]*Département de Chimie, Université de Montréal, C.P. 6128 Succursale A, Montréal, Québec H3C 3J7, Canada*

(Received 11 July 2016; accepted 13 September 2016; published online 30 September 2016)

We present a novel simple model to describe molecular photocells where the energy conversion process takes place by a single molecular donor-acceptor complex attached to electrodes. By applying quantum scattering theory, an open quantum system method, the coherent molecular photocell is described by a wave function. We analyze photon absorption, energy conversion, and quantum yield of a molecular photocell by considering the effects of electron-hole interaction and non-radiative recombination. We model the exciton creation, dissociation, and subsequent effects on quantum yield in the energy domain. We find that depending on the photocell structure, the electron-hole interaction can normally decrease or abnormally increase the cell efficiency. The proposed model helps to understand the mechanisms of molecular photocells, and it can be used to optimize their yield. *Published by AIP Publishing.* [http://dx.doi.org/10.1063/1.4963335]

I. INTRODUCTION

Photovoltaic energy is a fascinating and promising response to the challenge of green renewable energy. Small molecule organic photocells consist of single molecules or molecular complexes that are subjected to sunlight and attached to electrodes. Because of significant advantages, such as flexibility, relatively simple synthesis, high charge carrier mobility, and low cost, molecular photocells, have been considered[1–4] as one of the various promising photovoltaic technologies. Several groups[5–8] have investigated coherently controlled molecular junctions, which are very similar to the systems examined here.

In molecular photocells, following the photon absorption, electron-hole pair creation occurs in a confined zone,[9–12] and hence, the Coulomb interaction between the charge carriers and the associated recombination plays an essential role.[13–17]

While understanding the performance of organic photovoltaic cells has been a central effort of the scientific community for many years,[18–24] theoretical approaches facilitating the understanding of electron-hole interaction and recombination effects on molecular photocell performance are needed. Semi-classical theories are inefficient tools to treat interaction problems in nanostructure-based solar cells,[25,26] and on the other hand, due to the Coulomb attraction between the photo-generated carriers, the application of standard Non-Equilibrium Green Function (NEGF) theory presents some difficulties although some specific methods allow circumventing this problem.[7]

We develop an approach, which is based on scattering theory and provides a simple alternative method to treat realistic situations with electron-hole interaction and recombination. In this formalism, the central quantity is a wave function, which represents the operation of molecular photocell. The wave function consists of two components: the first one shows the system in its ground state before photon absorption and the second one which is called scattered wave function ($|\Psi_P(E)\rangle$) represents the charge carriers photo-generated by absorption of a photon with energy E. The electric field generated by incident photons couples these two components.

By knowing $|\Psi_P(E)\rangle$, one can compute the fluxes of absorbed photons, of recombined electron-hole pairs, and of charges injected in the evacuation channels. The determination of these quantities gives access to a detailed analysis of the photocell performance. The effects of electron-hole interaction, recombination rate, and of the coupling strength to the different evacuation channels on the quantum yield can be examined. Let us emphasize that the results presented here do not treat the effect of an external varying voltage. In that sense, we are not presenting a full theory of a two-level solar cell. Yet the present work sheds light on basic quantum phenomena that occur in this type of cell.

It is worthwhile to note that the modern experimental techniques such as the one explored in Refs. 27–31 should be suitable to realize single-molecule photocells. We expect that experimental techniques can be developed that retain the simple mechanism explored in this manuscript.

The paper is organized as follows. In Section II, the theoretical model for a two-level system is outlined. In Section III, various illustrations of our model, discussing

a)Author to whom correspondence should be addressed. Electronic mail: tahereh.nematiaram@neel.cnrs.fr

the parameterization effects, are provided. The conclusions are given in Section IV.

II. THEORETICAL MODEL FOR A TWO-LEVEL MOLECULAR PHOTOCELL

A. Basic concepts

The basic idea of our methodology is described through the example of a two-level photovoltaic system with the electron-hole interaction and non-radiative recombination. This two-level system is characterized by the HOMO (highest occupied molecular orbital) and the LUMO (lowest unoccupied molecular orbital) of the molecule coupled to the charge evacuation channels that represent the electrodes (Fig. 1, Left).

Initially, the whole system is in the ground state with filled valence bands and empty conduction bands. After photon absorption by the molecule, one electron and one hole are created in LUMO and HOMO, respectively. Both charge carriers interact via the Coulomb potential and can be recombined in the molecule or can be transferred to their respective channels where they produce photovoltaic current.

In this model, the energy difference between LUMO and HOMO levels is equal to Δ. The coupling matrix elements between the molecular states and the possible evacuation channels in materials I and II are denoted by m. The hopping matrix element inside each evacuation channel is considered uniform and denoted by t. The onsite energies of the electron at position (x) and the hole at position (y) are assumed to be $\varepsilon_e(x)$ and $\varepsilon_h(y)$, respectively. The Coulomb attractive potential with strength U represents the presence of local-interaction between the electron and the hole when they are both inside the molecule.

The Hilbert space of such a structure can be mapped onto a square lattice where x (y) represents the position of the electron (hole), in the molecule or in the attached chains (Fig. 1, Right). Site $x = 0$ corresponds to the LUMO orbital in the molecule and $x > 0\,(x < 0)$ represents the position of the electron in its respective chains in material I (material II). Similarly, for $y = 0$, the hole is in the HOMO and $y > 0\,(y < 0)$ corresponds to the sites of the effective chains in material II (material I). Therefore, site $(x = 0, y = 0)$ corresponds to the electron–hole pair localised on the molecule and it represents the initial state just after the absorption of a photon. Application of the tight binding method[32] to the mentioned 2D square lattice can construct the effective Hamiltonian of the system,

$$H = \sum_i \varepsilon_i |i\rangle\langle i| + \sum_{i,j} t_{ij} |i\rangle\langle j| . \tag{1}$$

Here the first term indicates the total onsite energy of each square lattice basis state which is defined as a summation over the electron onsite energy, the hole onsite energy, and the Coulomb interaction energy between them,

$$\varepsilon(x, y) = \varepsilon(x) + \varepsilon(y) + U. \tag{2}$$

Since we study the effect of local attractive Coulomb interaction, U is allowed to take negative non-zero values only if the electron and the hole are inside the molecule, i.e., on the site (0, 0). Furthermore, the probability of photogenerated electron-hole pair local-recombination inside the molecule is taken into account by adding an imaginary part $-i\Gamma_R/2$ to the onsite energy of the site (0, 0), where Γ_R is the recombination probability parameter.

Finally, the second term in Equation (1) represents the coupling energy between two successive basis states on the square lattice (Fig. 1, right). As pointed above, the coupling energies between molecular state (i.e., site (0, 0)) and its first neighbours are different from that of the other coupling energies.

By knowing the effective Hamiltonian of the system and starting from the quantum scattering theory and the Lipmann-Schwinger equation,[33] we introduce the scattered electron-hole pair wave function $|\Psi_P(E)\rangle$ which is defined on the square lattice and allows computing all the required fluxes to analyze the quantum yield of the cell,

$$|\Psi_P(E)\rangle = \frac{1}{z - H} |0,0\rangle . \tag{3}$$

Here $z = E + i\varepsilon$ is a complex energy with an infinitesimal positive imaginary part ε. As explained previously, $|0,0\rangle$ represents the excited state consisting of an electron-hole pair inside the molecule that is created by absorption of the photon. To have an idea about the behavior of scattered wave

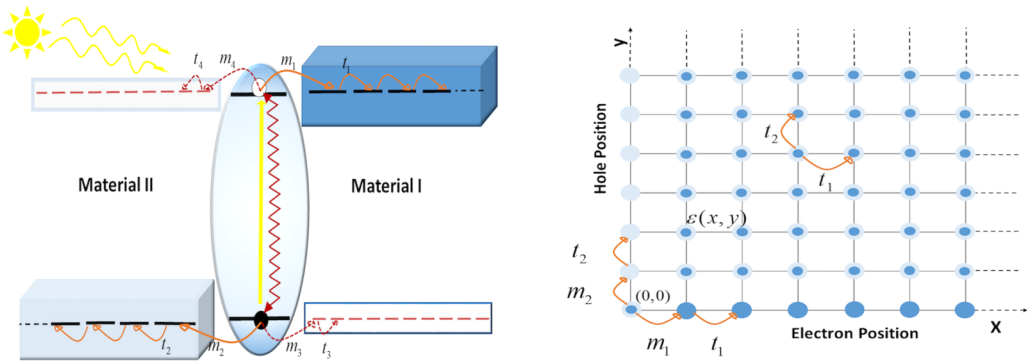

FIG. 1. (Left) The two-level model for a molecular photocell with one HOMO and one LUMO orbitals attached to the electrodes in materials I (right) and II (left). The wiggly line represents the electron-hole interaction and recombination inside the molecule and the hopping integrals of electron and hole are denoted by m and t. (Right) The square lattice representation by considering just one evacuation channel for each charge carrier, with one state at each point (x, y) of the lattice. The coordinates x and y of a given state represent the position of electron and hole in their respective channels. $\varepsilon(x, y)$ is the onsite energy of each site of the square lattice and the hopping integrals (m and t) are along the bonds of the square lattice.

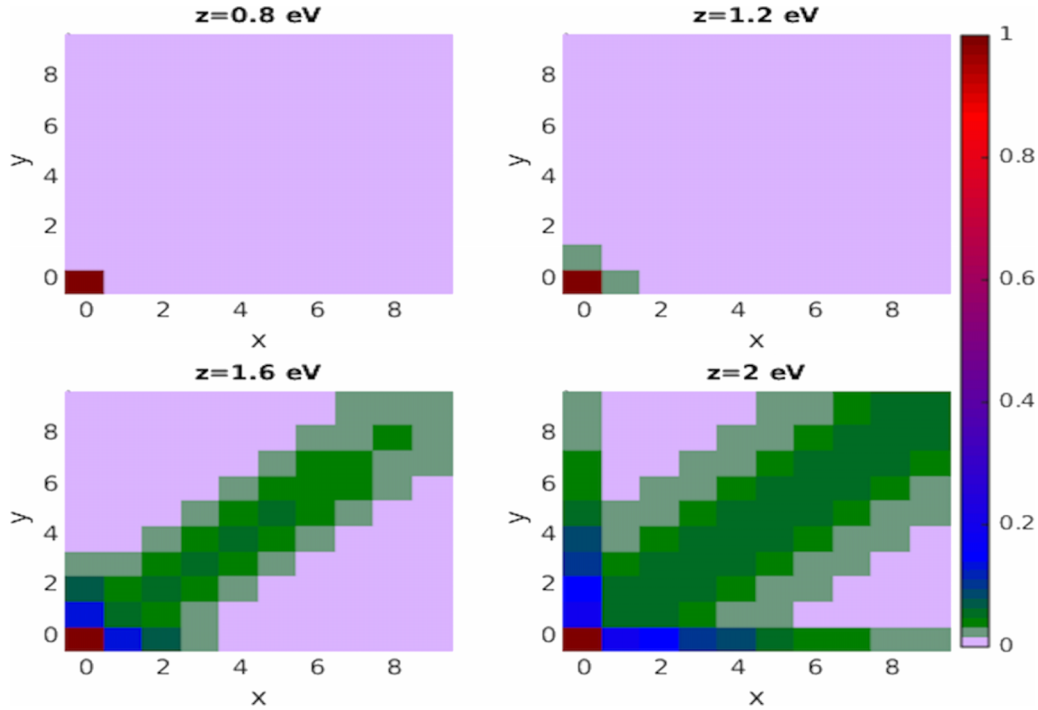

FIG. 2. Weight of the scattered wave function ($|\Psi_P(E)\rangle$) on different sites (x,y) of the square lattice normalized to its value on the initial site ($|\langle x,y|\Psi_P(E)\rangle|^2/|\langle 0,0|\Psi_P(E)\rangle|^2$) for various absorbed photon energies (z). The cell parameters are $t_1 = t_2 = 0.2$ and $m_1 = m_2 = 0.1$, and the energy difference between the LUMO and HOMO energy levels (Δ) is equal to 2; therefore, the energy continuum (EC) is between 1.2 and 2.8 (all energies are in eV unit).

function ($|\Psi_P(E)\rangle$), Fig. 2 represents the weight of $|\Psi_P(E)\rangle$ on different sites (x,y) of the square lattice normalized to its value on the initial site $\left(\frac{|\langle x,y|\Psi_P(E)\rangle|^2}{|\langle 0,0|\Psi_P(E)\rangle|^2}\right)$ by considering various absorbed photon energies (z) for a cell with energy continuum (EC) lying between 1.2 and 2.8 eV. Since we represent the electron-hole pair by a wave-function, we can consider this model as a coherent model. Yet as discussed above, we can include the effect of recombination through an imaginary part of the energy on site (0, 0) which represents the electron and the hole in the molecule.

By applying the Born approximation, which is valid for sufficiently low illumination intensity, for any physical quantity measured by an operator A, one has

$$\langle A(E)\rangle = \alpha^2(E)\langle\Psi_P(E)|A|\Psi_P(E)\rangle\,. \tag{4}$$

$\alpha^2(E)$ is the product of the square of the dipole matrix element of the molecular transition d times the electromagnetic energy density $\rho(E)$ of photons with energy E, i.e.,

$$\alpha^2(E) = \frac{d^2\rho(E)}{2\varepsilon_0}, \tag{5}$$

where ε_0 is the vacuum permittivity.

B. Fluxes and quantum yield

The cell performance can be described through the definition of a series of fluxes. The incoming flux of photons $\Phi_{ph}(E)$ is defined as a number of absorbed photons per unit time and it is related to $n(E)$ the local density of states (LDOS's) on the site $|0,0\rangle$ through

$$\Phi_{ph}(E) = \alpha^2(E)\frac{2\pi}{\hbar}n(E). \tag{6}$$

Equation (4) is equivalent to Fermi's golden rule and $n(E)$ is given by

$$n(E) = \frac{1}{\pi}\frac{(\Gamma_R + \Gamma_P(E))}{(E - \Delta - U - E_P(E))^2 + (\Gamma_R + \Gamma_P(E))^2}, \tag{7}$$

where U ($U < 0$) and Γ_R are the electron-hole interaction energy and the recombination rate inside the molecule, respectively. $E_P(E)$ and $\Gamma_P(E)$ are the real and imaginary parts of the self-energy of site $|0,0\rangle$ (i.e., the molecule in its excited state). For sufficiently small coupling between molecule and the channels (small m values compared to bandwidth), the value of $n(E)$ is important only near the resonance energy E_{res} such that

$$E_{res} \approx E(0,0) = \Delta + U. \tag{8}$$

Δ is the energy difference between HOMO and LUMO. $E(0,0)$, which is the on-site energy of the state (0,0) of the square lattice, represents the excitation energy of the molecule and plays an important role here.

We introduce $\Phi_R(E)$ and $\Phi_P(E)$ which are the fluxes of pairs that recombine in the molecule and pairs that escape from the molecule, respectively. Their ratio is given by the ratio between recombination and escaping rates. Based on the flux conservation, one has $\Phi_{Ph}(E) = \Phi_R(E) + \Phi_P(E)$; therefore, the flux of outgoing charges can be related to the total photon flux through the equation

$$\Phi_P(E) = \Phi_{Ph}(E) \times \frac{\Gamma_P(E)}{\Gamma_R + \Gamma_P(E)}. \tag{9}$$

This formula has a classical form but let us recall that the different rates are computed through a quantum model. The current intensity in material I induced by photons of energy E

is $I(E) = -e\,\Phi_C(E)$, where $-e$ is the electron charge. $\Phi_C(E)$ is defined by

$$\Phi_C(E) = \Phi_P(E)R(E). \tag{10}$$

In this equation, $R(E) = p_{e1}(E) - p_{h1}(E)$ where $p_{e1}(E)$, and $p_{h1}(E)$ are the proportion of electrons and holes evacuated from the molecule to the channel in material I. $R(E)$ is computed from the electron-hole pair scattered wave function and a simple analytical expression can be extracted in the wide band limit (i.e., $m_n < t_n$),

$$R(E) \approx \left(\frac{\Gamma_{eI}}{\Gamma_{eI}+\Gamma_{eII}} - \frac{\Gamma_{hI}}{\Gamma_{hI}+\Gamma_{hII}}\right). \tag{11}$$

$\Gamma_{eI/hI/hII}$ are the injection rates of electrons or holes (e/h) in material I/II. Again this formula has a classical form but the different rates are computed through a quantum model. By combining Equations (4)-(9), one obtains an expression for $I(E) = -e\,\Phi_C(E)$ which generalizes the formula obtained in Ref. 34 (see the supplementary material),

$$\Phi_C(E) = \alpha^2(E)\frac{2}{\hbar}\left[\frac{\Gamma_P}{(E-\Delta-U)^2+(\Gamma_R+\Gamma_P)^2}\right] \times \left[\frac{\Gamma_{eI}}{\Gamma_{eI}+\Gamma_{eII}} - \frac{\Gamma_{hI}}{\Gamma_{hI}+\Gamma_{hII}}\right]. \tag{12}$$

This equation, comprising the effects of electron-hole interaction (U) and recombination rate (Γ_R), is an extension of the formula obtained in Ref. 34 for non-interacting and non-recombining electron-hole pairs. The interaction energy (U) shifts the resonance energy at which photons are absorbed and the recombination processes (Γ_R) decrease the total amount of current injected in the channels. Note that the relative proportion of charge carriers injected in the different channels are unchanged by the local interaction and local recombination processes.

At a given photon energy E, the yield $Y(E)$ is defined as a ratio between the number of electron charges injected in material I to the total number of absorbed photons $Y(E) = \Phi_C(E)/\Phi_{Ph}(E)$.

Based on the equation mentioned before, one obtains

$$Y(E) = \left(\frac{\Gamma_P(E)}{\Gamma_R+\Gamma_P(E)}\right) \times R(E). \tag{13}$$

In this article, we take $\alpha^2(E) = \alpha^2$ in the region, where $n(E)$ (i.e., photon absorption) is important.

The total flux of absorbed photons is equal to $\Phi_{ph} = \int \Phi_{ph}(E)dE = 2\pi\alpha^2/\hbar$. This quantity depends only on the light intensity and dipole matrix element of the molecular transition. On the other hand, the total flux injected in material I, $\Phi_C = \int \Phi_C(E)dE$ depends on the parameters of the cell. The average yield (Y) is defined as

$$Y = \frac{\Phi_C}{\Phi_{Ph}} = \int n(E)Y(E)dE. \tag{14}$$

If $n(E)$ (i.e., photon absorption) is significant in a narrow region around the energy E_{res}, then $Y \approx Y(E_{res})$. Based on Equation (11), $Y(E_{res})$ depends not only on the ratio between recombination and escaping rates Γ_R and $\Gamma_P(E_{res})$, but also on $R(E_{res})$.

III. RESULTS AND DISCUSSIONS

To illustrate various aspects of the model, we consider a two-level system in two different configurations: (A) mono-channel case where there is just one possible evacuation channel for each charge carrier (i.e., m_1 & $m_2 \neq 0$). (B) Multi-channel case where there are evacuation channels in materials I and II for the hole while there is just one evacuation channel in material I for the electron (i.e., m_1 & m_2 & $m_3 \neq 0$). Here, the widths of the energy continuum EC_1 (electron injected in material I and hole in material II) and EC_2 (electron and hole injected in material I) are the important parameters and they play an essential role. Hence, in the multi-channel case, we investigate the performance of the system under two specified conditions: (B1) multi-channel system with identical energy continuums (i.e., $EC_1 = EC_2$) and (B2) multi-channel system with different energy continuums (i.e., $EC_1 \neq EC_2$).

Note that when the electron and the hole are far away from the molecule, they do not interact. This means that there is a continuum of pair states such that their energies are the sum of the electron and the hole energies in their respective channels. By this consideration, one can determine the width and edges of energy continuums EC_1 and EC_2 from the spectrum of electrons and holes in their respective leads.

By energy conservation, a photon of energy E can generate a pair far away from the molecule only if E represents a given energy in the continuum EC. We vary the electron-hole interaction strength U, the recombination rate Γ_R, and the coupling parameters m_n ($n = 1, 2, 3$) to analyse their impact on the electronic structure and charge separation yield.

A. Mono-channel system

In this case, we use $t_1 = t_2 = 0.2$ and $\Delta = 2$; therefore, the energy continuum lies between 1.2 and 2.8 eV. In addition, $R(E) = p_{e1}(E) - p_{h1}(E)$, which represents the proportion of electrons and holes evacuated from the molecule to the channel in material I, is equal to one. In Fig. 3, the LDOS is plotted as a function of the absorbed photon energy.

In these plots, the dependence of LDOS on local interaction energy (U), strength of coupling parameters (m), and recombination rate (Γ_R) is examined. As can be seen from panels (a) and (b), for a given set of coupling parameters and in the absence of recombination, the number of LDOS peaks is dependent on the interaction strength. For small values of $|U|$, there is a single peak which tends to become narrower for larger $|U|$. The peak eventually splits into two for growing values of $|U|$ and the resulting two peaks separate further with increasing $|U|$ as depicted in panel (b). The narrow peak outside the continuum (EC) is called excitonic state, which blocks the charge carrier injection to the energy continuum.

Next, we study the effects of the coupling parameters. The corresponding LDOS is shown in panel (c). Increasing m enhances charge carrier transfer from HOMO and LOMO to the respective evacuation channels; it can be detected through the extended width of the LDOS line shape. In panel (d), the effect of varying the recombination rate (Γ_R) for interacting and non-interacting cases is shown. In both cases, the effect

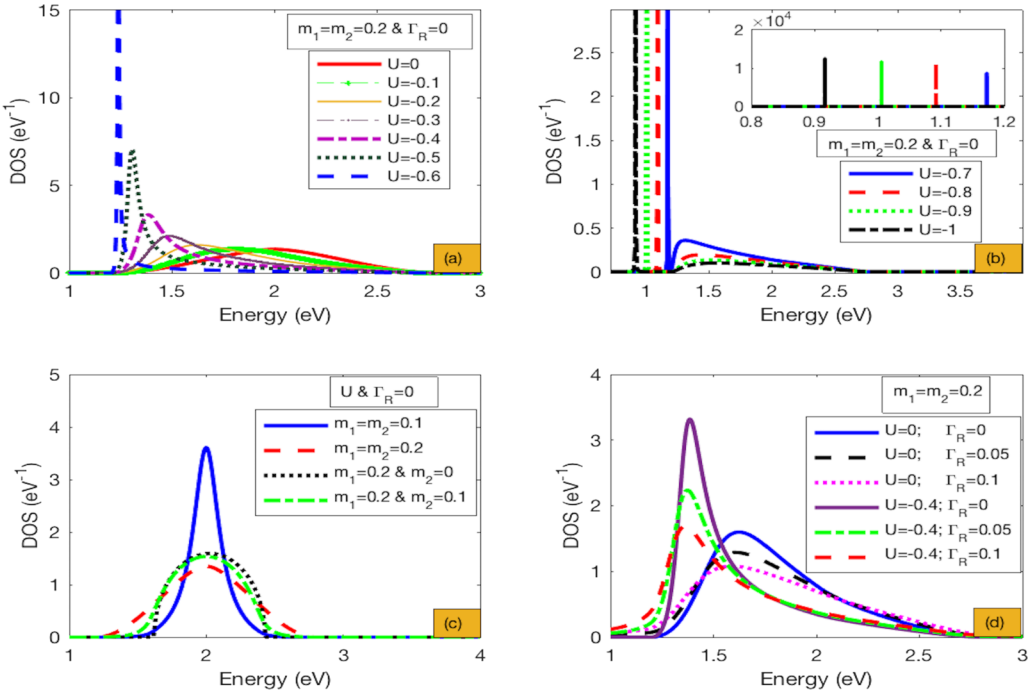

FIG. 3. Density of states as a function of incident photon energy in a mono-channel system under different conditions. ((a) and (b)) For different values of interaction energy (U). (c) For different coupling parameters (m_1 & m_2). (d) For different interaction energies and recombination rates (U, Γ_R).

of Γ_R is to slightly shift the LDOS line shape to the left and to slightly broadening of the line shape width.

Figure 4 shows the dependence of the yield Y on the electron-hole interaction (U) and recombination rate (Γ_R) for different set of coupling parameters (m_1 and m_2). In all cases, for small values of interaction energy, the yield remains 1 for $\Gamma_R = 0$. The effect of Γ_R and U is to reduce the yield. This behaviour can be understood based on the information provided in Fig. 3. For larger values of $|U|$, the charge carriers will stay on the molecule to form a localized state because their energy does not lie in the energy continuum of the contacts.

For large values of the coupling parameters (m_1 and m_2), more charge carriers will transfer to the evacuation channels

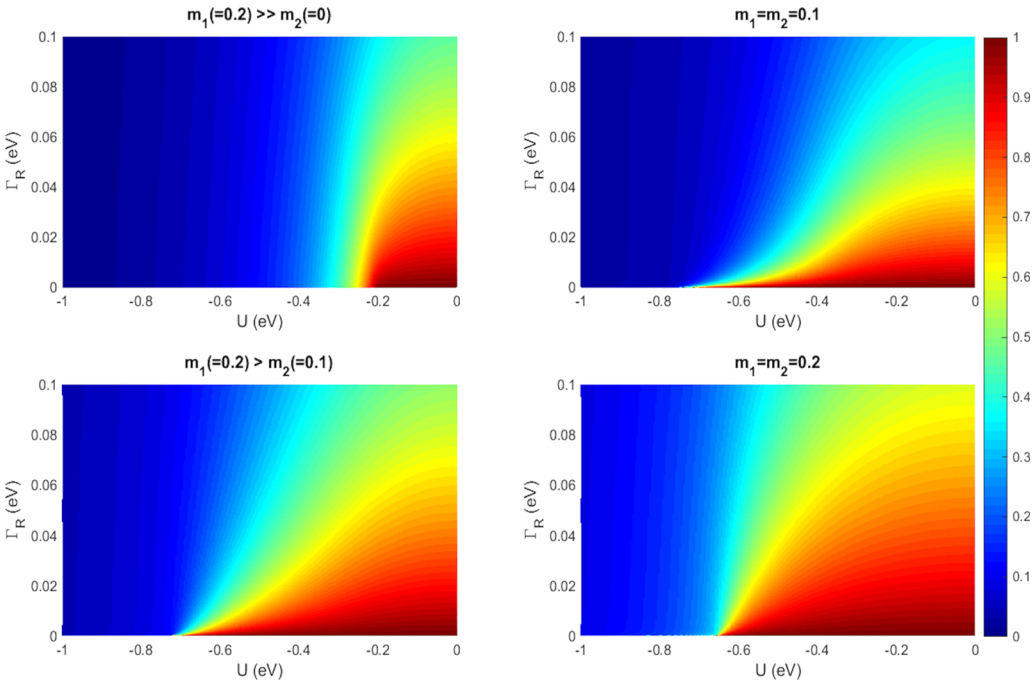

FIG. 4. Photovoltaic yield as a function of interaction energy (U) and recombination rate (Γ_R) in a mono-channel system for different values of coupling parameters (m_1 and m_2).

and hence the cell remains efficient over a wider range of the recombination parameter.

B. Multi-channel system

In the following, the process of charge separation is studied by considering coupling to two different evacuation channels for the hole and only one evacuation channel for the electron. The system performance is investigated by considering first two identical and then two different energy continuums.

1. Multi-channel system with two identical energy continuums

In Fig. 5, charge separation yield as a function of interaction energy (U) and recombination rate (Γ_R) and corresponding LDOS as a function of absorbed photon energy are examined by considering two energy continuums (EC_1 and EC_2) with identical bandwidths.

The cell parameters $t_1 = 0.2$, $t_2 = 0.4$, $t_3 = 0.4$, $m_1 = 0.2$, and $\Delta = 2$ are kept constant whereas m_2 and m_3 are varied. Therefore, EC_1 and EC_2 are between 0.8 and 3.2 eV. Here, $R(E)$ given by $R(E) = m_2^2/m_2^2 + m_3^2$ is energy independent (see the supplementary material). Similar to the mono-channel case, the yield decreases when $|U|$ or Γ_R increases. Based on the spectral information provided in the second row of this figure, due to the electron–hole interaction, charge carriers tend to localize to form an exciton outside the energy continuums, and by increasing $|U|$, more charge carriers will be localized.

Therefore, the charge separation yield remains one until creation of localized state and increasing the coupling parameters of HOMO to material II will lead to higher values of $R(E)$ and increase the yield.

2. Multi-channel system with two different energy continuums

Next, in Fig. 6, LDOS and the corresponding charge separation yield are examined by considering two energy continuums (EC_1 and EC_2) with different bandwidths. The cell parameters $t_1 = 0.2$, $t_2 = 0.4$, $t_3 = 0.1$, $m_1 = 0.2$, and $\Delta = 2$ are kept constant whereas m_2 and m_3 are varied. As depicted in panel (a), for small values of $|U|$, E_{res} falls within EC_1 and EC_2; hence, holes can be injected in materials I and II, depending on the values of the coupling parameters.

With increasing $|U|$, E_{res} is outside the EC_2 while it is within the EC_1. Therefore, regardless of the strength of the coupling parameter, the hole will be evacuated only in material II. Finally, for strong enough U, E_{res} is outside the two continuums and charge carriers will be localized inside the molecule.

In panels (b) and (c), for $U = -1$, the effects of varying m_2 and m_3 are examined. Their influences are detected by

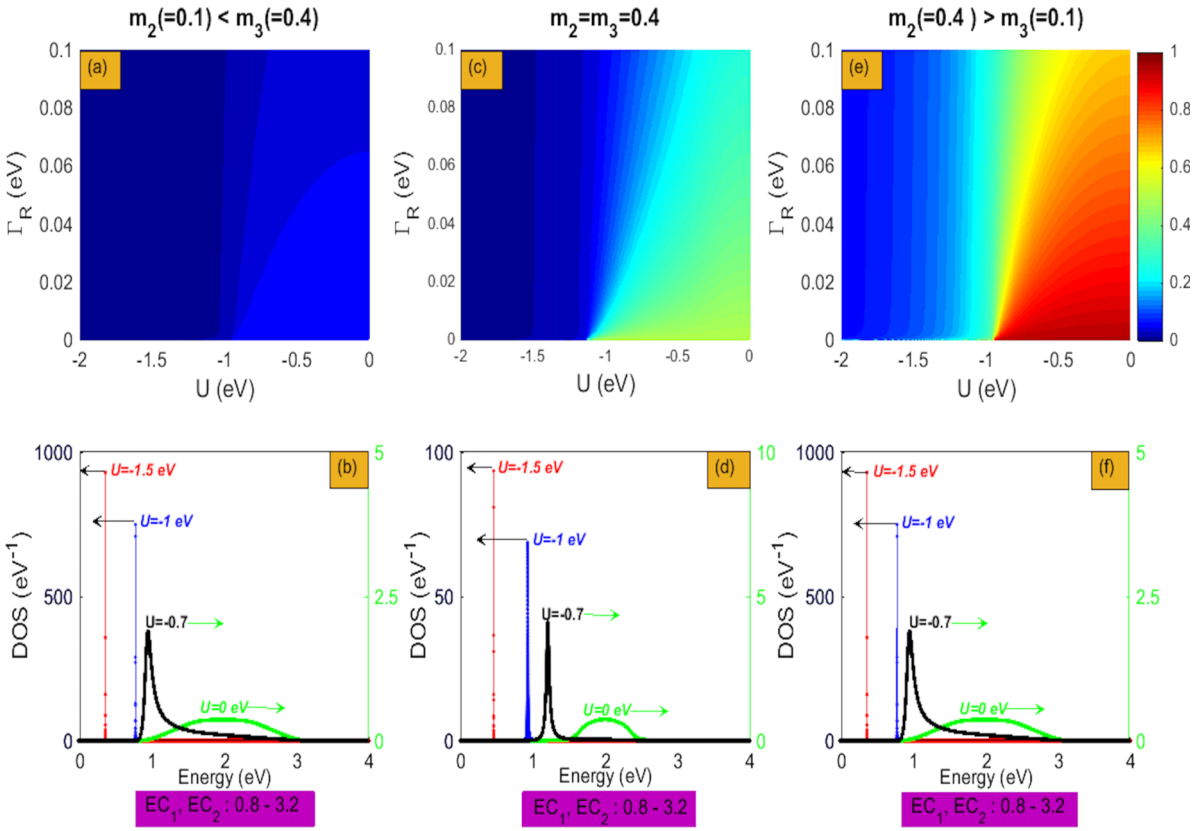

FIG. 5. Photovoltaic yield and LDOS in a multi-channel system with identical energy continuums. ((a), (c), and (e)) Photovoltaic yield as a function of interaction energy (U) and recombination rate (Γ_R) for different values of coupling parameters of the hole to material II and material I (m_2 & m_3). ((b), (d), and (f)) DOS as a function of incident photon energy for different values of interaction energy. The energy continuum range is indicated by coloured band below the DOS plots.

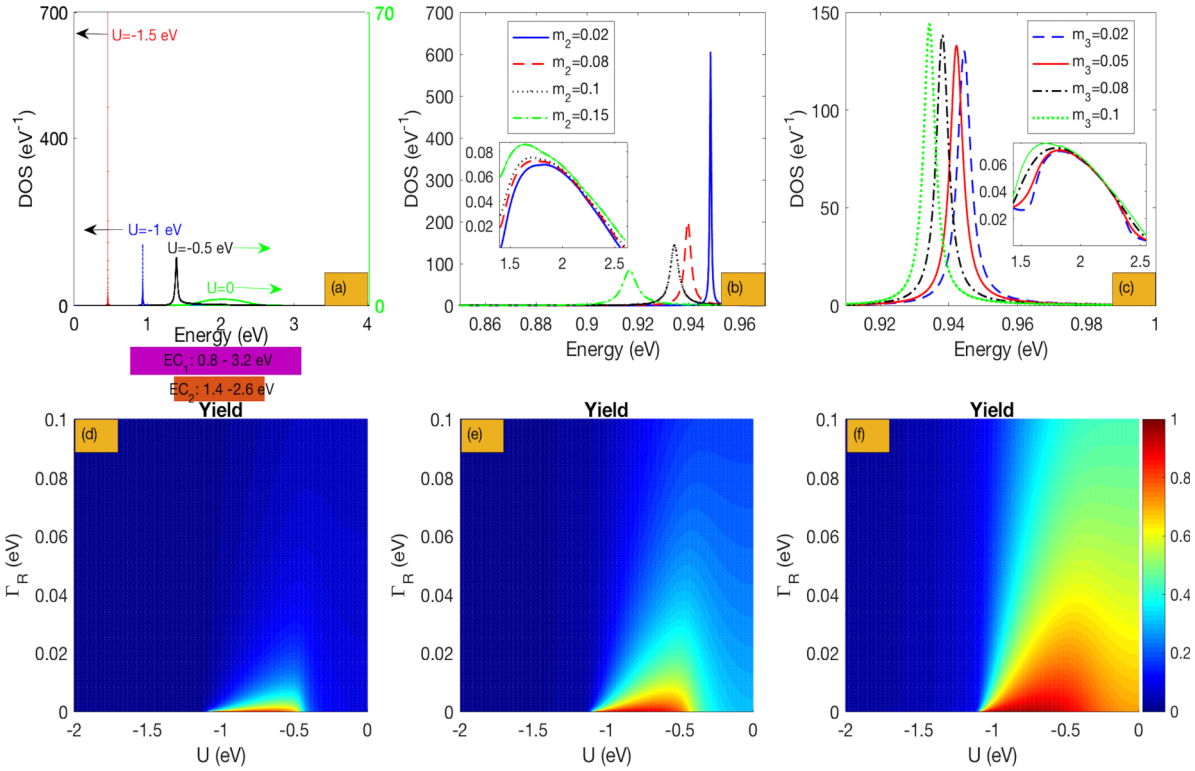

FIG. 6. LDOS and yield in a multi-channel system with different energy continuums. (a) DOS as a function of absorbed photon energy for different values of U. The energy continuums EC_1 (electron in material I and hole in material II) and EC_2 (electron and hole in material I) ranges are shown by colored bands below the plot. Here, $m_2 = m_3 = 0.1$. (b) LDOS computed for $m_3 = 0.1$, $U = -1$, and different values of m_2. (c) LDOS computed for $m_2 = 0.1$, $U = -1$, and different values of m_3. ((d)–(f)) Photovoltaic yield in a multi-channel system with different energy continuums as a function of interaction energy (U) and recombination rate (Γ_R) for different values of coupling parameters of the hole to material II and material I (m_2 and m_3).

changing the position of resonance energy (E_{res}) and width of the line shape. In the figure inset the behaviour of the line shape inside the second energy continuum (EC_2) is shown. As can be seen, the variation inside the EC_2 is negligible. This behaviour is understandable by referring to level repulsion.[35] Spectral information shown through Figures 6(a)-6(c) provides an appropriate framework to interpret the behaviour of the photocell yield.

Through panels (d-f) in Fig. 6, we examine the yield by taking three different sets of HOMO coupling parameters to material I and material II (m_2 and m_3).

The yield variations can be understood by separation of the interval of charge interaction energy (U) into three zones. The first zone considers $U \in [0, -0.5]$, where the resonance energy is coupled to two continuums EC_1 and EC_2; therefore, the coupling parameters determine the appropriate channel and the yield values. As can be seen, the cell can be efficient in this range of U if and only if $m_2 \geq m_3$. The maximum value of the yield in all cases is detected in the interval of $U \in [-0.5, -1.1]$. Based on the spectral information (Fig. 6(a)), in this range of U values, the resonance energy just lies in the continuum EC_2; therefore, the hole either jumps into material II or stays at the molecule. Increasing m_2 enhances the yield. For larger interaction parameter values, $U \in [-1.1, -2]$, the resonance energy does not lie in any continuum; therefore, the yield of the cell tends to be zero. In addition, the effect of the recombination rate (Γ_R) is to reduce the yield.

IV. CONCLUSIONS

We have presented a theoretical model based on the wave function of a coherent molecular photocell. This theory is well adapted to analyse molecular photocells in the presence of strong Coulomb interaction between the electron and the hole. We show that there is a competition between injection of charge carriers in the leads and recombination. This competition depends sensitively on the parameters of the model such as the local electron-hole interaction in the molecule, the recombination rate, the coupling to the leads, and the band structure of the leads. When there are several evacuation channels for the charge carriers (electrons or holes), there is, in addition, a competition between injections in the different channels. Although some of the results presented here show similarity with kinetic models, the value for the final current and therefore the cell efficiency can be obtained only through a complete *quantum* calculation.

The formalism can also be applied to molecules with more complex electronic structures. This method should help to understand the conditions needed for a high yield of a molecular photovoltaic system, such as single molecule junctions or a molecular monolayer.

SUPPLEMENTARY MATERIAL

See supplementary material for the complete explanation of the formalism.

ACKNOWLEDGMENTS

The authors would like to thank Daniel Lincot, Jean-François Guillemoles, Emilio Lorenzo, Simone Fratini, and Kevin-davis Richler for fruitful discussion and careful reading of the manuscript. In addition, the financial support provided by Campus France and Institut Néel is acknowledged.

[1]C. J. Brabec, "Organic photovoltaics," Sol. Energy Mater. Sol. Cells **83**, 273 (2004).
[2]M. T. Lloyd, J. E. Anthony, and G. G. Malliaras, Mater. Today **10**, 34 (2007).
[3]M. Grätzel, Nature **414**, 338 (2001).
[4]K. A. Mazzio and C. K. Luscombe, Chem. Soc. Rev. **44**, 78 (2015).
[5]R. Volkovich and U. Peskin, Phys. Rev. B **83**, 033403 (2011).
[6]U. Peskin and M. Galperin, J. Chem. Phys. **136**, 044107 (2012).
[7]A. J. White, U. Peskin, and M. Galperin, Phys. Rev. B **88**, 205424 (2013).
[8]Y. Selzer and U. Peskin, J. Phys. Chem. C **117**, 22369 (2013).
[9]D. Cahen, G. Hodes, M. Grätzel, J. F. Guillemoles, and I. Riess, J. Phys. Chem. B **104**, 2053 (2000).
[10]J. L. Brédas, J. E. Norton, J. Cornil, and V. Coropceanu, Acc. Chem. Res. **42**, 1691 (2009).
[11]S. Ten Cate *et al.*, J. Phys. Chem. Lett. **4**, 1766 (2013).
[12]F. Yang and S. R. Forrest, ACS Nano **2**, 1022 (2008).
[13]S. Westenhoff *et al.*, J. Am. Chem. Soc. **130**, 13653 (2008).
[14]R. A. Street, M. Schoendorf, A. Roy, and J. H. Lee, Phys. Rev. B **81**, 205307 (2010).
[15]R. A. Street, Phys. Rev. B **84**, 075208 (2011).
[16]Y. Yi, V. Coropceanu, and J. L. Brédas, J. Am. Chem. Soc. **131**, 15777 (2009).
[17]I. Mora-Sero *et al.*, Acc. Chem. Res. **42**, 1848 (2009).
[18]S. Ajisaka, B. Žunkovič, and Y. Dubi, Sci. Rep. **5**, 8312 (2015).
[19]M. Einax, M. Dierl, and A. Nitzan, J. Chem. Phys. **115**, 21396 (2011).
[20]M. Einax and A. Nitzan, J. Chem. Phys. **145**, 014108 (2016).
[21]M. Einax and A. Nitzan, J. Phys. Chem. C **118**, 27226 (2014).
[22]T. N. Aram, A. Asgari, and D. Mayou, EPL **115**, 18003 (2016).
[23]S. Fratini, D. Mayou, and S. Ciuchi, Adv. Funct. Mater. **26**, 2292 (2016).
[24]S. Ciuchi, S. Fratini, and D. Mayou, Phys. Rev. B **83**, 081202 (2011).
[25]Z. Arefinia and A. Asgari, Sol. Energy Mater. Sol. Cells **137**, 146 (2015).
[26]A. V. Semichaevsky and H. T. Johnson, Sol. Energy Mater. Sol. Cells **108**, 189 (2013).
[27]S. Battacharyya *et al.*, Nano Lett. **11**, 2709 (2011).
[28]J. A. Fereiro, R. L. McCreery, and A. J. Bergren, J. Am. Chem. Soc. **135**, 9584 (2013).
[29]Y. Furmansky *et al.*, J. Mater. Chem. **22**, 20334 (2012).
[30]S. V. Aradhya and L. Venkataraman, Nat. Nanotechnol. **8**, 399 (2013).
[31]D. Gerster *et al.*, Nat. Nanotechnol. **7**, 673 (2012).
[32]P. Vogl, H. P. Hjalmarson, and J. D. Dow, J. Phys. Chem. Solids **44**, 365 (1983).
[33]L. L. Foldy and W. Tobocman, Phys. Rev. **105**, 1099 (1957).
[34]M. Galperin and A. Nitzan, Phys. Rev. Lett. **95**, 206802 (2005).
[35]P. Von Brentano, Phys. Lett. B **238**, 1 (1990).